International Journal of Advancements in Electronics & Electrical Engineering– IJAEEE 2018
Copyright © Institute of Research Engineers and Doctors , SEEK Digital Library
Volume 6 : Issue 2 [ISSN : 2319-7498] - Publication Date: 25 June , 2018

Full-scale BRRP seismic dampers

Tsutomu Usami

]

***Abstract*—A further study is presented on developing a high-performance full-scale seismic damper, named Buckling Restrained Rippled Plate (BRRP) damper. BRRPs are to be installed at the edges of a girder-type bridge, acting as energy dissipating seismic dampers for severe earthquakes. Cyclic loading tests have confirmed that the tested BRRPs perform well and fulfill specified performance requirements.**

Keywords- seismic damper, buckling restrained rippled plates, cyclic test, analysis

I. Introduction

Full-scale metallic seismic dampers termed buckling-restrained rippled plate (BRRP) dampers [1], using a rippled plate with out-of-plane bucking restrained by restraining components illustrated in Fig.1 are to be developed. This type of dampers can be installed at two directions, i.e., the axial direction and the corresponding perpendicular direction to control the movement at the ends of a girder-type bridge [1].

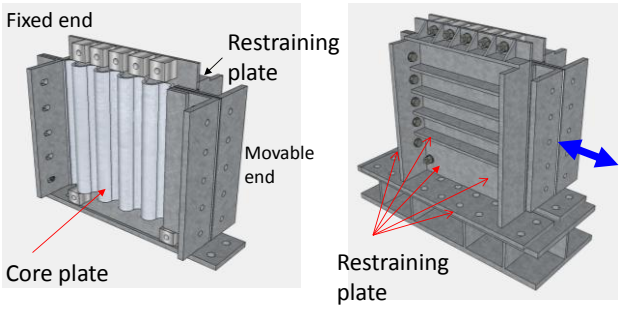

(a) Restraining plate on one side (b) Restraining plate on two sides

Fig.1 Overall view of test specimens

Based on the achievements of the previous paper [1], this paper aims to develop full-scale BRRP dampers with the following expected characteristics using both experimental and numerical approaches: 1) a load-carrying capacity over 400kN; 2) a deformation capacity over 40mm; 3) local strain below 4% to 5%. The first two targets are demanded based on seismic response of a 30m simply supported steel girder bridge with two BRRP dampers at its each end, where the response is under the Japanese Level 2 earthquake [2]. The pertinent research project includes the following two items: 1) performance verification using cyclic tests (capacity tests) under variable- and constant-amplitude loading protocols; 2) seismic evaluation of simply supported steel girder bridges with BRRP dampers at the two ends using pseudo-dynamic tests (demand tests). In this paper only the first item is presented because of the limitation of space. For the numerical simulations, nonlinear elasto-plastict analyses under cyclic loading are conducted using shell models.

Tsutomu Usami
Emeritus Professor of Nagoya University
Nagoya, Japan.
e-mail: usamit@meijo-u.ac.jp

II. Performance tests and numerical analyses

The performance requirements [3], i.e., deformation capacity and low cycle fatigue performance of BRRPs through both full-scale cyclic loading tests and numerical analyses are investigated. The deformation capacity is described by the maximum displacement, Δ_u, at the movable end of a BRRP, and the low cyclic fatigue performance is evaluated by the limit value of the cumulative inelastic strain, CID_{lim}, where the average strain, Δ/L_0, is employed during the calculation of the two indices.

A. *Outline of tests*

Three specimens made of SS400 (Japan Industrial Standard (JIS) designation) with the same configuration shown in Fig.2 and listed in Table 1 were manufactured, where Specimens No.1 and No.2 were respectively under cyclic variable- and constant-amplitude loading. In Table 1, r/t = ratio of the internal curvature radius of the core plate to the plate thickness; d = distance between the two restraining plates; d_0 = gap between the external surface of the core plate and the

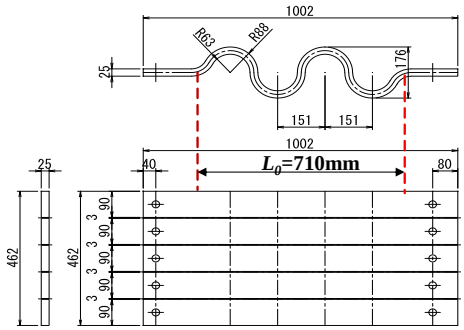

Fig.2 Core rippled plate

International Journal of Advancements in Electronics & Electrical Engineering– IJAEEE 2018
Copyright © Institute of Research Engineers and Doctors , SEEK Digital Library
Volume 6 : Issue 2 [ISSN : 2319-7498] - Publication Date: 25 June , 2018

Table 1 List of test specimens

No..	r/t	t (mm)	gap (mm)	L_0 (mm)	Δ_m (mm)	Δ_{y0} (mm)	$2A$ (mm)	$d/2A$	Loading condition
1	2.5	25	d=192 d_0=8	710	40	7.0	151	1.27	Variable amplitude
2						—			Constant amplitude

Table 2 Tension coupon test results

	Specimen No.	t (mm)	r/t	E (GPa)	σ_y (MPa)	ε_y (%)	E_{st} (GPa)	ε_{st} (%)	σ_u (MPa)	δ_u (%)	v
After stamping	No.1	25	2.5	205	361	0.176	3.13	0.87	469	23.8	0.28
	No.2	25	2.5	192	416	0.217	3.08	0.80	520	19.6	0.28

E=Young's modulus, σ_y =yield stress, ε_y=yield strain, E_{st}=strain-hardening modulus, ε_{st}= strain at onset of strain hardening, σ_u=tensile strength, δ_u=elongation, , v=Poisson's ratio

internal surface of the restraining plate; L_0 = length of the deformable portion (Fig,2); Δ_m = designed displacement limit; Δ_{y0} = yield displacement to decide the loading protocol; $2A$ = the height between the centerlines of the two neighboring wave crests. For all the specimens, the displacement limit, ultimate load and local strain targets are respectively set as 40mm, 400 kN and 4% to 5% according a process presented in the previous study [1]. Blocking phenomenon due to expansion of the rippled core plate under compression can occur in BRRPs [1]. To avoid or reduce this unfavorable result, the value of d_0 were determined according to the preliminary numerical analyses,

The experiments were conducted using a large-scaled loading device at Meijo University, and the test setup as illustrated in Figs.3. The horizontal load was applied along the mid-height center line of the specimen using an actuator with a load capacity of ±1000 kN fixed at a reaction column of a self-balanced loading frame.

Specimen No.1 was loaded with cyclic loading history at an amplitude interval of Δ_{y0} as listed in Table 1. The constant displacement amplitude for Specimen No.2 is designed as ±40 mm, which is the designed displacement limit, and the experiment is expected to be terminated when the load decreases by 20%. This test is aimed to investigate the low cycle fatigue properties of the BRRP under constant amplitude loading history.

The net horizontal displacement of the rippled core plate is obtained by excluding the average displacement at the fixed end, the slip of the base plate and the deformation of the fixed end from the average horizontal displacement of the movable end. The strain data along the loading direction are also measured utilizing a type of large plastic deformation capacity strain gauge with a gauge length of 2 mm. The distribution and numbering of strain gauge locations is given in Fig.4. Four gauges are mounted at each concave surface of the wave crests, (G_1 to G_4), where the strain data are the largest, and totally 16 gauges are employed for each rippled plate.

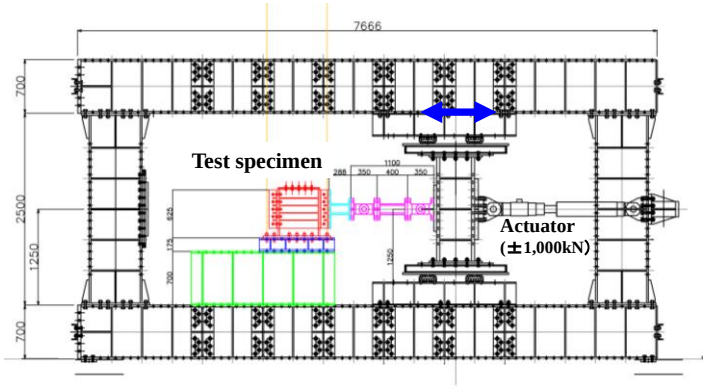

Fig. 3 Test setup

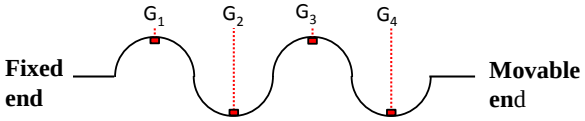

Fig. 4 Strain-gauge locations

B. *Test results*

Tension coupons manufactured before and after the stamping of the rippled core plate were both tested as in the previous study [1]. The obtained material mechanical properties after stamping are presented in Table 2.

The experimental load-horizontal displacement hysteretic curve of Specimen No.1 is shown in Fig.5(a). A stabilized spindle-shaped hysteretic curve is obtained, which is favorable for seismic dampers. The maximum tensile load equals 460 kN, and the maximum compressive tensile load reaches 423kN, where both are larger than the target load-carrying capacity, 400kN. The maximum horizontal displacement, Δ_u, reaches the designed displacement limit, Δ_m, which equals ±40 mm. Load decreasing due to damage of the core plates is not

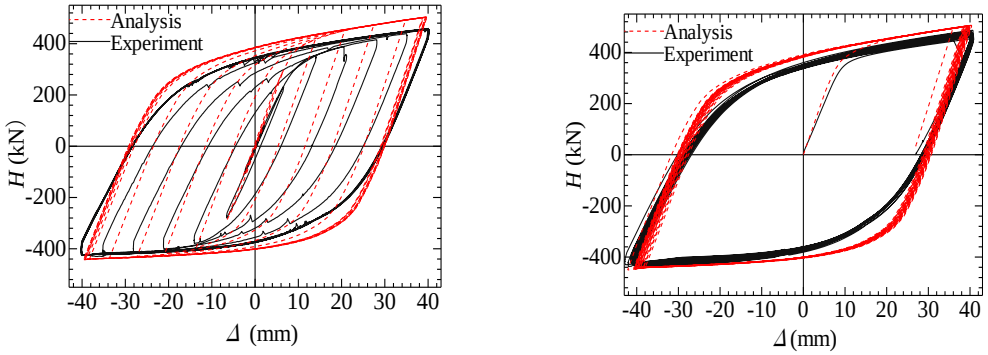

(a) Test specimen No.1 (b) Test specimen No.2

Fig.5 Comparison of the experimental and analytical *H-Δ* relationships

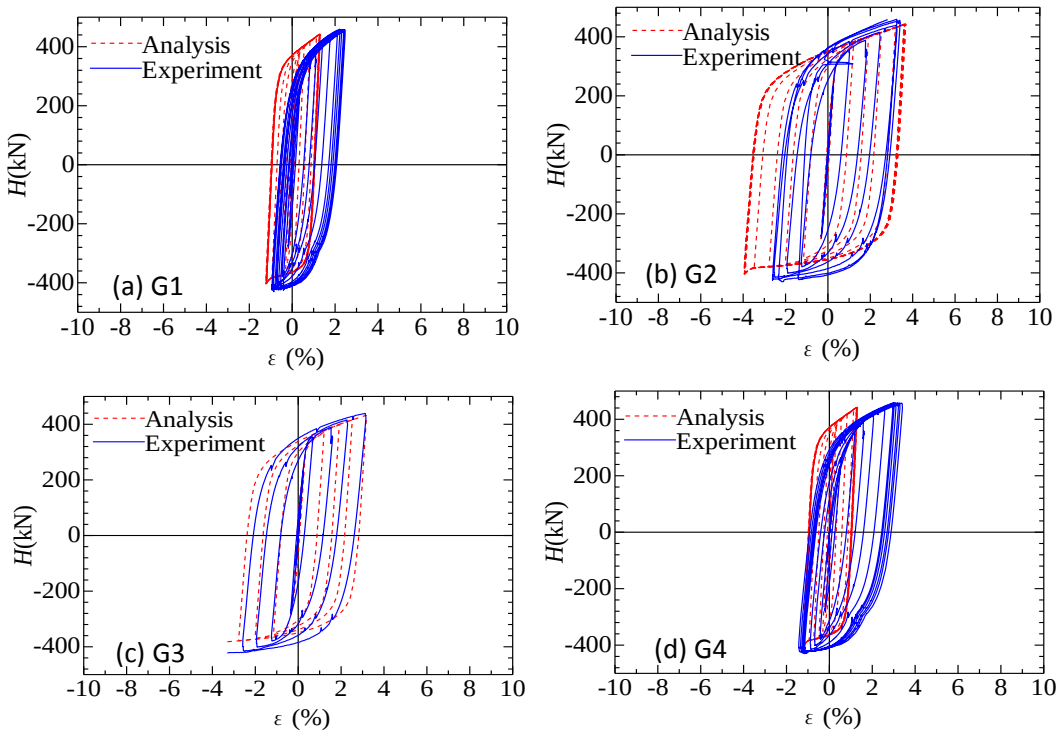

Fig. 6 Comparison of the experimental and analytical *H-local strain* relation

observed at the instant when Δ_m is reached. The specimen was loaded under the constant amplitude of ±40 mm. The experiment was finally terminated due to rotation of the hinge at the loading beam close to the movable end after 9 cycles of constant amplitude cyclic loading.

The measured local strain data at the locations G_1 to G_4 shown in Fig.4 are plotted against the horizontal load in Fig.6. From the figures, it has been observed that the strains at the center (G2 and G3) are larger than those close to the movable and fixed ends (G4 and G1), while the formers are still smaller than the maximum average strain, Δ_u/L_0=±5.63% .As presented before, an interesting as well as important phenomenon that the local strains are smaller than the average strain has been demonstrated. In addition, the strain data are all found below the target value of 4% to 5%.

International Journal of Advancements in Electronics & Electrical Engineering– IJAEEE 2018
Copyright © Institute of Research Engineers and Doctors , SEEK Digital Library
Volume 6 : Issue 2 [ISSN : 2319-7498] - Publication Date: 25 June , 2018

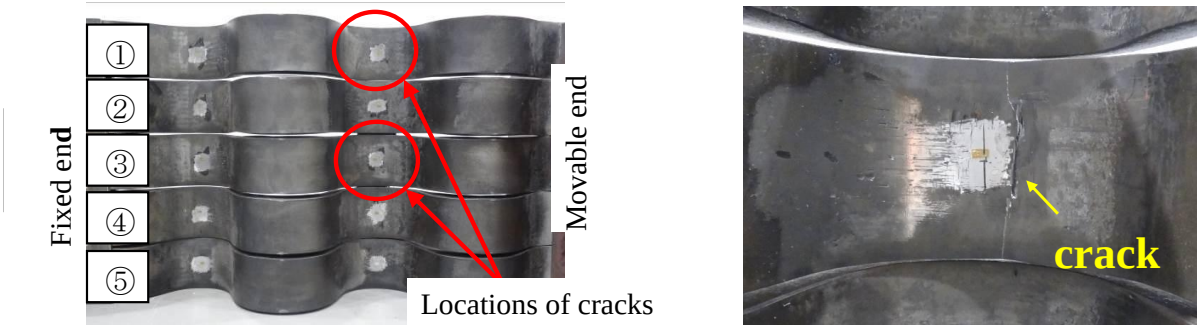

(a) Overall view (b) Close-up view of crack on plate ③

Table 7 Test specimen after low-cycle fatigue failure（Test specimen No.2）

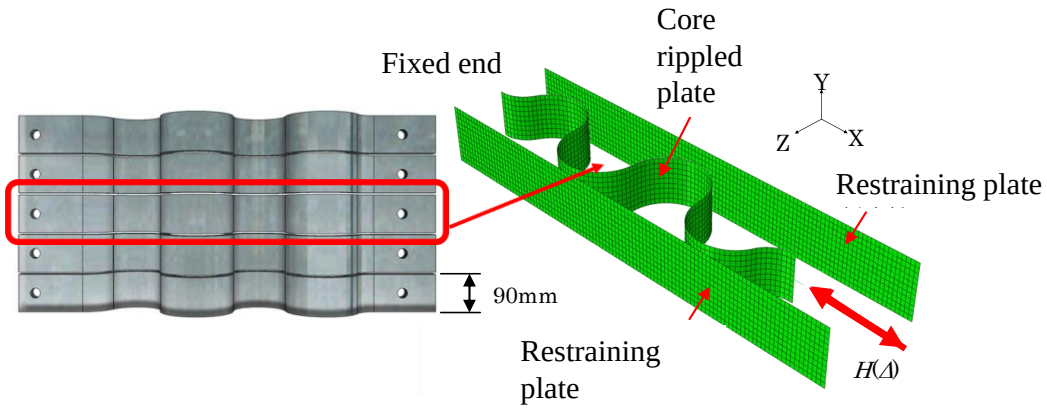

Fig. 8 Analytical model of BRRP

The employed amplitude of Specimen No.2 is ±40 mm, and the horizontal load-horizontal displacement curve is plotted in Fig.5(b). A stabilized spindle-shaped hysteretic curve is obtained, and the target load-carrying capacity is also achieved. Increase of the maximum load is only observed in the second cycle, and the maximum load decreases slightly for the subsequent loading cycles. The experiment was terminated due to low cycle fatigue fracture of the core plate at the 32th loading cycle as shown in Figs.7. Low cycle fatigue fracture is observed at the second wave of the core plates, and crack propagates apparently at the center core plate.

The performance indices are all listed in Table 3, including the deformation capacity index, i.e., maximum average strain, Δ_u/L_0; the maximum local strain, ε_u; the low cycle fatigue performance index, i.e., the cumulative inelastic strain, CID_{lim} and the maximum load, H_u. The values for CID_{lim} obtained from the subsequent numerical analyses are also given in the table. The maximum average strain and the cumulative inelastic strain are respectively employed as the index of the deformation capacity of BRRPs and the low cycle fatigue performance. Great deviation is observed for the cumulative inelastic strains of Specimens No.1 and No.2 listed in Table 3.

Table 3 Capacity of test specimens

No.	Δ_u/L_0	H_u (kN)		ε_u (%)		CID_{lim}	
		T	C	T	C	test	analysis
1	0.0563	460	-430	4.39	-3.84	1.80	1.96
2	0.0563	487	-437	5.58	-4.66	5.40	5.76

Note: T=tension side, C=compression side

This is mainly for that the failure of Specimen No.2 is caused by low cycle fatigue, while Specimen No.1 fails due to rotation at the movable end prior to the low-cycle fatigue failure of the test specimen. Therefore, the values of the indices of Specimen No.1 in Table 3 are actually not the deformation capacity or the low cycle fatigue capacity of the seismic dampers given in the literature [3]. However, the incremental amplitude loading test is more realistic compared with the one under constant amplitude loading considering the actual loading history in severe seismic events. In addition, utilizing the incremental amplitude loading for the evaluation of the capacity is conservative. Thus, the test results of Specimen No.1 are employed as the capacities of the performance indices in the safety evaluation studies [5], which are not shown in this paper due to the space limitation.

C. *Outline of numerical analysis*

The numerical model is shown in Fig.7, where one of the five rippled core plates with a height of 90 mm, a thickness of 25 mm and a length of L_0=710 mm was simulated. The boundary conditions are the same as those in the previous study [1], where the translational freedom along the Y direction was constrained. The core plate was simulated using shell elements (S4R) in Abaqus program, and the restraining plates were postulated as rigid plates. Enforced cyclic horizontal displacements were applied to the movable end to carry out nonlinear elasto-plastic cyclic loading analyses. Bilinear kinematic hardening rules with the second branch hardening modulus E / 100 (E is the Young's modulus) were employed. The model parameters were calibrated from the post-stamping coupon test results listed in Table 2. Contact between the core plate and the restraining plates were judged by the centerlines of the shell elements in the previous study [1], while it is judged according to the external surfaces of the shell elements in the present study. The frictional coefficient is assumed to be 0.1. The residual stress and strain were not considered in the simulations for the application of the heat-treatment, and initial imperfection was also not introduced.

III. Comparison of experimental and numerical results

The horizontal load-horizontal displacement curves obtained from the numerical simulations are compared with the experimental ones in Figs.5.

The numerical results can generally compare well with the experimental ones.

Comparisons of horizontal load-local strain curves between the experiments and the simulations are presented in Figs.6. The figure indicates that shift of strain to the tensile side observed in the experiments is not reproduced by the simulations, and relatively large deviations are found at the gauges close to the fixed and movable ends (G1 and G4). On the other hand, the strain data at the centers of the numerical simulations can compare well with the experimental ones for the minor strain shift effect at the locations. Further studies on the causes of the strain shift are required, and more elaborate modeling of the BRRPs will also be necessary.

IV. Conclusions

As a subsequent study of the previous paper [1], a series of studies on seismic performance of full-scale BRRP dampers are carried out using cyclic loading tests (capacity tests), pseudo-dynamic tests (demand tests) and numerical analyses, aiming to develop a new type of high-performance dampers. Because of the space limitation, pseudo-dynamic tests are not included in this paper, and are presented in Ref. [5].

The main conclusions obtained from the study are given as follows.

1) The horizontal load H-horizontal displacement Δ hysteretic curves are very stable, and the three targets of this study are all achieved.
2) The fact that the local strain of the BRRPs is smaller than the average strain (Δ / L_0), is verified through the tests, and analyses which is just the opposite for BRBs and SPDs [4].
3) The H-Δ hysteretic curves, cumulative inelastic deformation, *CID*, obtained from the numerical analyses can generally compare well with the test results.
4) The phenomenon that the strain data tend to shift to the tensile side during the cyclic loading tests has not been reproduced in the numerical simulation.

Acknowledgement

This research work was supported by JSPS KAKENHI Grant Number JP15H04035.

References

[1] S. Yamazaki, T. Usami, T. and T. Nonaka, "Developing a new hysteretic type seismic damper (BRRP) for steel bridges, Engineering Structures, 124, pp.286-301, 2016.
[2] Japan Road Association (JRA). Specifications for Highway Bridges, Part V. Seismic Design, Tokyo, Japan, 2012 (in Japanese).
[3] T. Usami. Guidelines for seismic and damage-control design of steel bridges, Gihodo-Shuppan, Tokyo, Japan, 2006 (in Japanese).
[4] T. Usami, M. Kato, A. Kasai, "Required performances for buckling-restrained braces as a structural control damper. Journal of Structural Engineering, JSCE, 50A, pp. 527-538, 2004 (in Japanese).
[5] H. Kato, T. Usami,, S. Yamazaki, S. Mori, T. Noro and H.B. Ge, "Research for developing prototype buckling-restrained rippled plate (BRRP) dampers, Journal of Structural Engineering, JSCE, 61A, pp.211-223, 2015 (in Japanese).